

## SUPPORTING INFORMATION

Targeting TRAF6 E3 ligase activity with a small molecule inhibitor combats autoimmunity

**Jara K. Brenke<sup>1</sup>, Grzegorz M. Popowicz<sup>2,3</sup>, Kenji Schorpp<sup>1</sup>, Ina Rothenaigner<sup>1</sup>, Manfred Roesner<sup>4</sup>, Isabel Meininger<sup>5#</sup>, Cédric Kalinski<sup>6</sup>, Larissa Ringelstetter<sup>1</sup>, Omar R'kyek<sup>7,8</sup>, Gerrit Jürjens<sup>7,8</sup>, Michelle Vincendeau<sup>5,9</sup>, Oliver Plettenburg<sup>7,8</sup>, Michael Sattler<sup>2,3</sup>, Daniel Krappmann<sup>5</sup> and Kamyar Hadian<sup>1\*</sup>**

<sup>1</sup>Assay Development and Screening Platform, Institute of Molecular Toxicology and Pharmacology, Helmholtz Zentrum München, Neuherberg, Germany; <sup>2</sup>Institute of Structural Biology, Helmholtz Zentrum München, Neuherberg, Germany; <sup>3</sup>Center for Integrated Protein Science Munich at Chair of Biomolecular NMR, Department Chemistry, Technische Universität München, Garching, Germany; <sup>4</sup>mroe-consulting, Eppstein, Germany; <sup>5</sup>Research Unit Cellular Signal Integration, Institute of Molecular Toxicology and Pharmacology, Helmholtz Zentrum München, Neuherberg, Germany; <sup>6</sup>Innovation Management, Helmholtz Zentrum München, Neuherberg, Germany; <sup>7</sup>Institute of Medicinal Chemistry, Helmholtz Zentrum München, Neuherberg, Germany; <sup>8</sup>Institute of Organic Chemistry, Leibniz Universität Hannover, Hannover, Germany; <sup>9</sup>Institute of Virology, Helmholtz Zentrum München, Neuherberg, Germany

Running title: Inhibition of TRAF6 activity counteracts autoimmunity

<sup>#</sup>Present address: AbbVie Deutschland GmbH, Wiesbaden, Germany

<sup>\*</sup>To whom correspondence should be addressed: Kamyar Hadian: Assay Development and Screening Platform, Institute of Molecular Toxicology and Pharmacology, Helmholtz Zentrum München GmbH, Neuherberg, Germany; [kamyar.hadian@helmholtz-muenchen.de](mailto:kamyar.hadian@helmholtz-muenchen.de); Tel. +49 89 3187 2664

# Figure S1

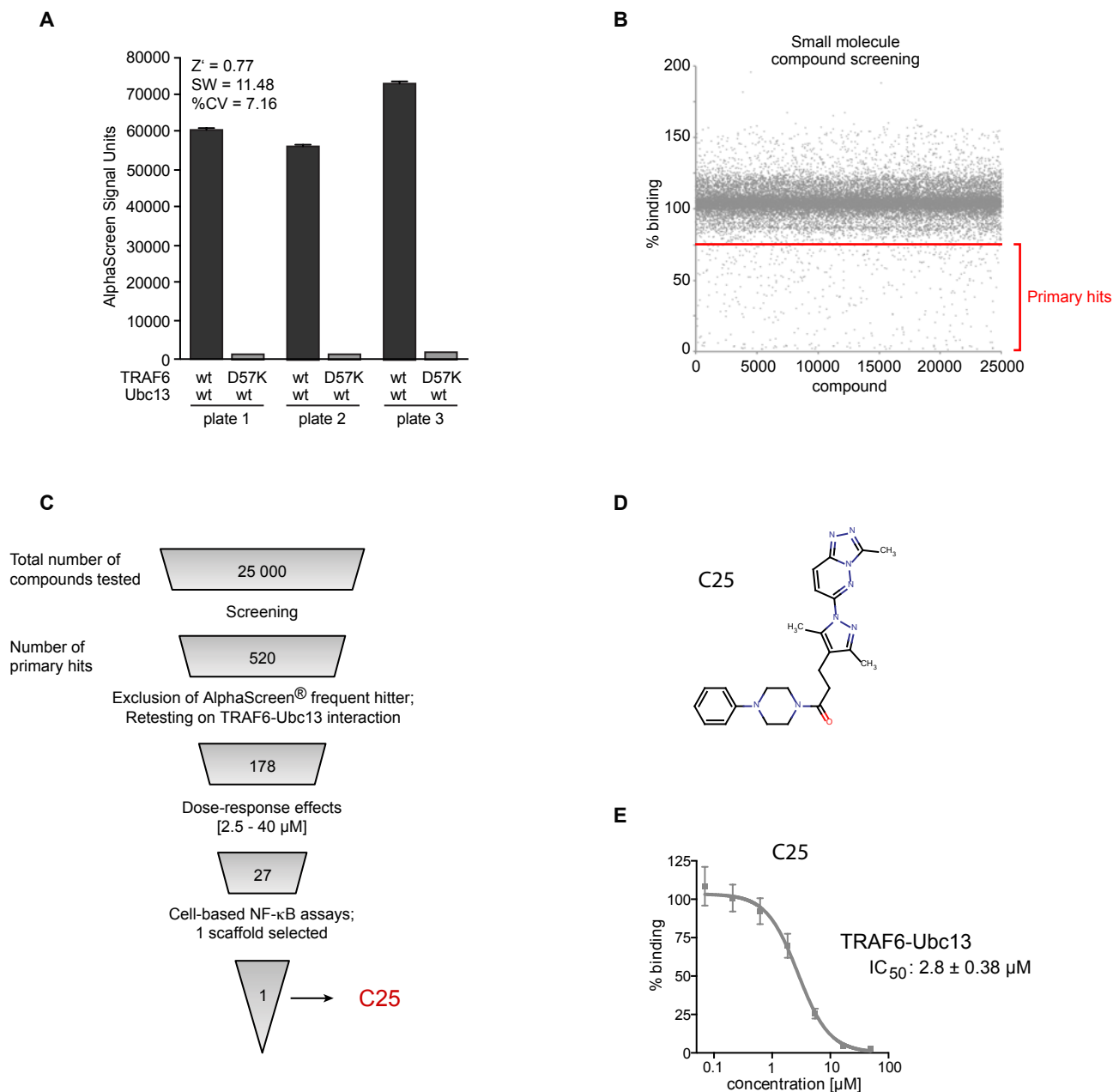
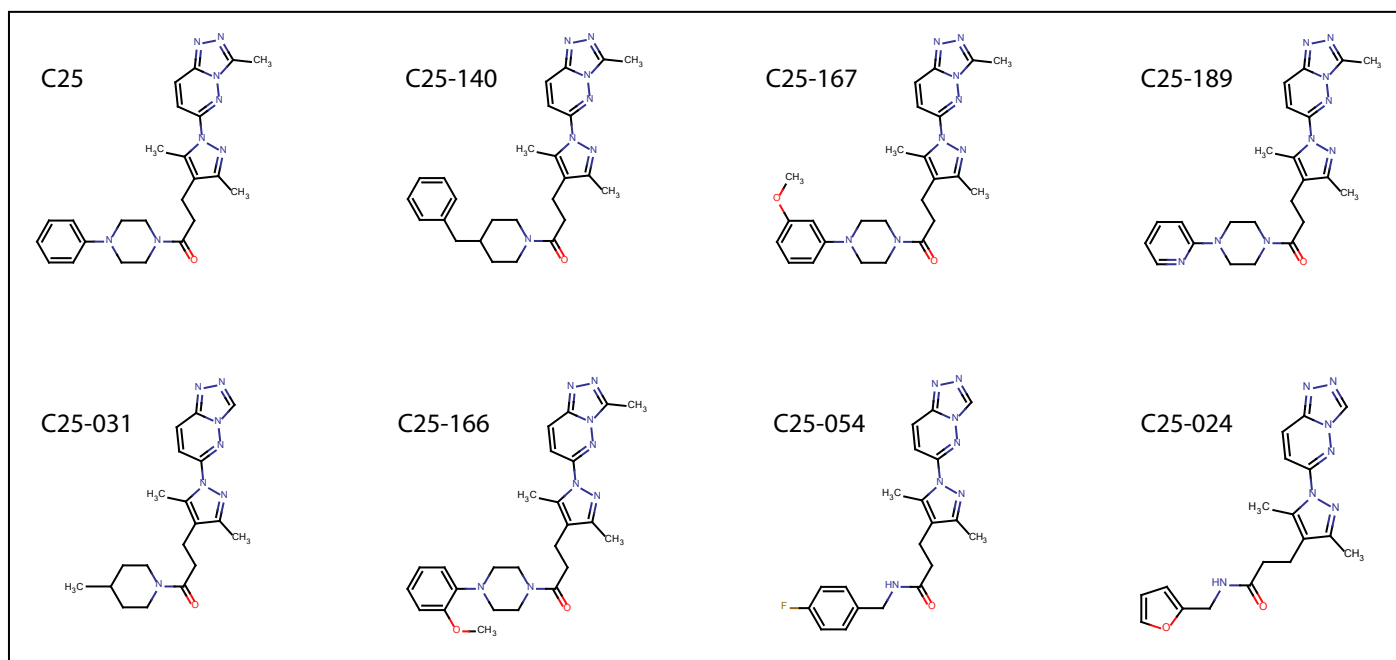


**Figure S1. Assay development, compound screening and hit selection to identify the first TRAF6-Ubc13 inhibitors.** *A*, AlphaScreen® assay using TRAF6 wt or D57K mutant proteins each in combination with Ubc13 wt. Assay was tested on three different plates to evaluate plate to plate variations. Statistical parameters for assay development ( $Z'$ , SW and %CV) are depicted. *B*, Output of the screening campaign using 25,000 compounds. Cut-off for compound selection was set to 75% binding. *C*, Step wise process to select compound C25-140 as the top hit for further evaluation. *D*, Structure of compound C25. *E*, Inhibition of TRAF6-Ubc13 by C25 in AlphaScreen® assays.

# Figure S2

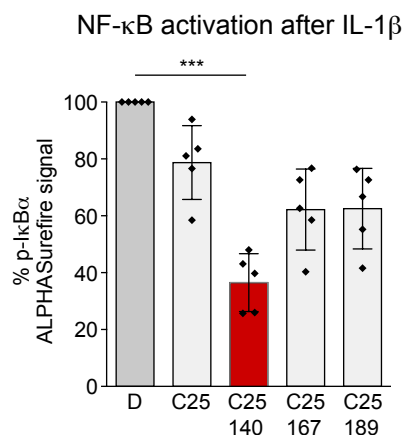
A



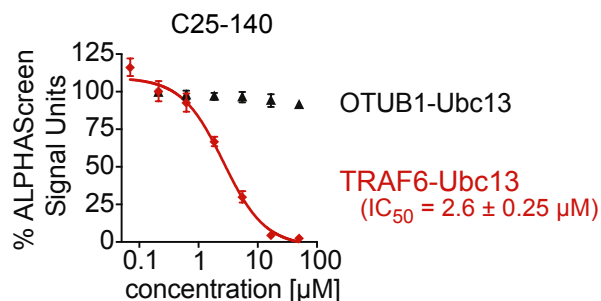
B

Compounds	IC <sub>50</sub> AlphaScreen
C25	2.8 ± 0.38 μM
C25-140	2.6 ± 0.25 μM
C25-167	1.5 ± 0.22 μM
C25-189	2.6 ± 0.25 μM
C25-031	> 40 μM
C25-166	> 40 μM
C25-054	> 40 μM
C25-024	> 40 μM

C



D



E

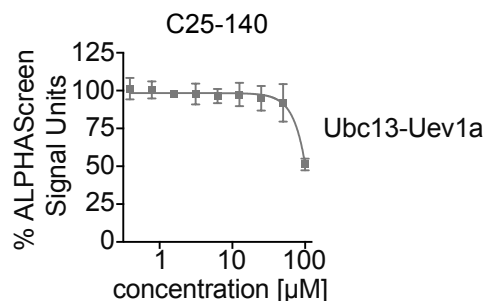


**Figure S2. Structure Activity Relationship (SAR).** A, Compound structures of C25 and 7 analogs. B, IC<sub>50</sub> values from AlphaScreen® assays for the 8 compounds depicted in A. C, Analysis of NF-κB activation after IL-1β stimulation using C25, C25-140, C25-167 and C25-189 each at 50 μM concentration. C25-140 has the best inhibitory potential. Error bars indicate mean ± S.D.; n = 5 biological replicates; unpaired t-test (two-tailed). \*\*\*P < 0.001. D, In AlphaScreen® assays, C25-140 inhibits TRAF6-Ubc13 binding, but not OTUB1-Ubc13 interaction. E, Interaction of Ubc13 with Uev1a is not affected by C25-140 in AlphaScreen® assays.

# Figure S3

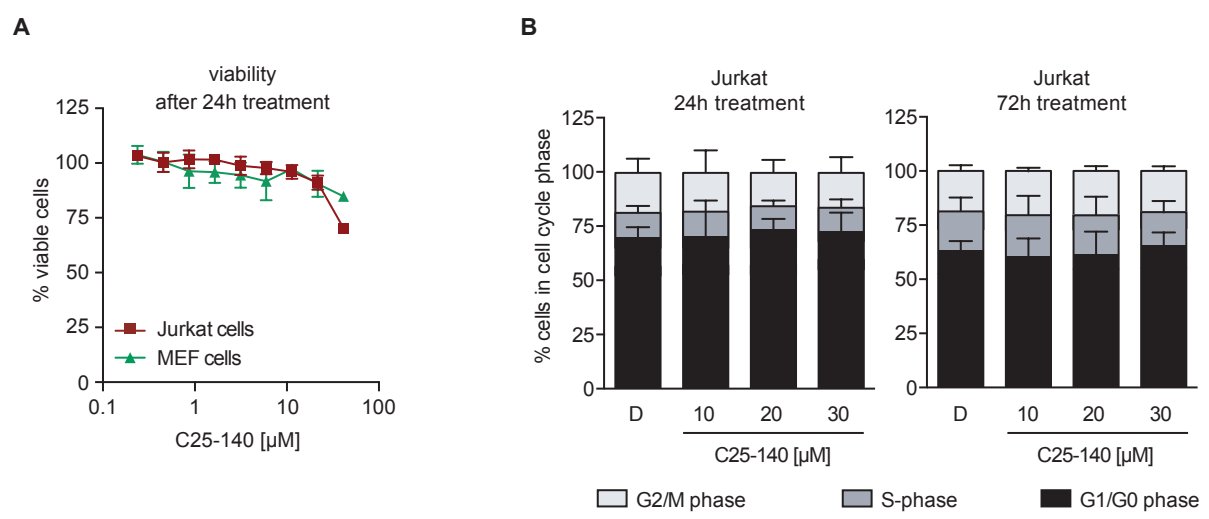


**Figure S3. C25-140 is not toxic and does not affect cell cycle phases.** A, Viability of MEF cells and Jurkat T-cells was evaluated after dose-dependent treatment of cells with C25-140 for 24h using the CellTiter-Glo assay that measures levels of cellular ATP (n = 3). No substantial signs of toxicity was evident. B, The effect of C25-140 on cell cycle was investigated after propidium iodide staining of Jurkat T-cells and subsequent analysis of the cell cycle phases by flow cytometry. 24 and 72 hours treatment had no effect on the cell cycle (n=3). Error bars indicate mean +/- S.D.; D = DMSO

# Figure S4

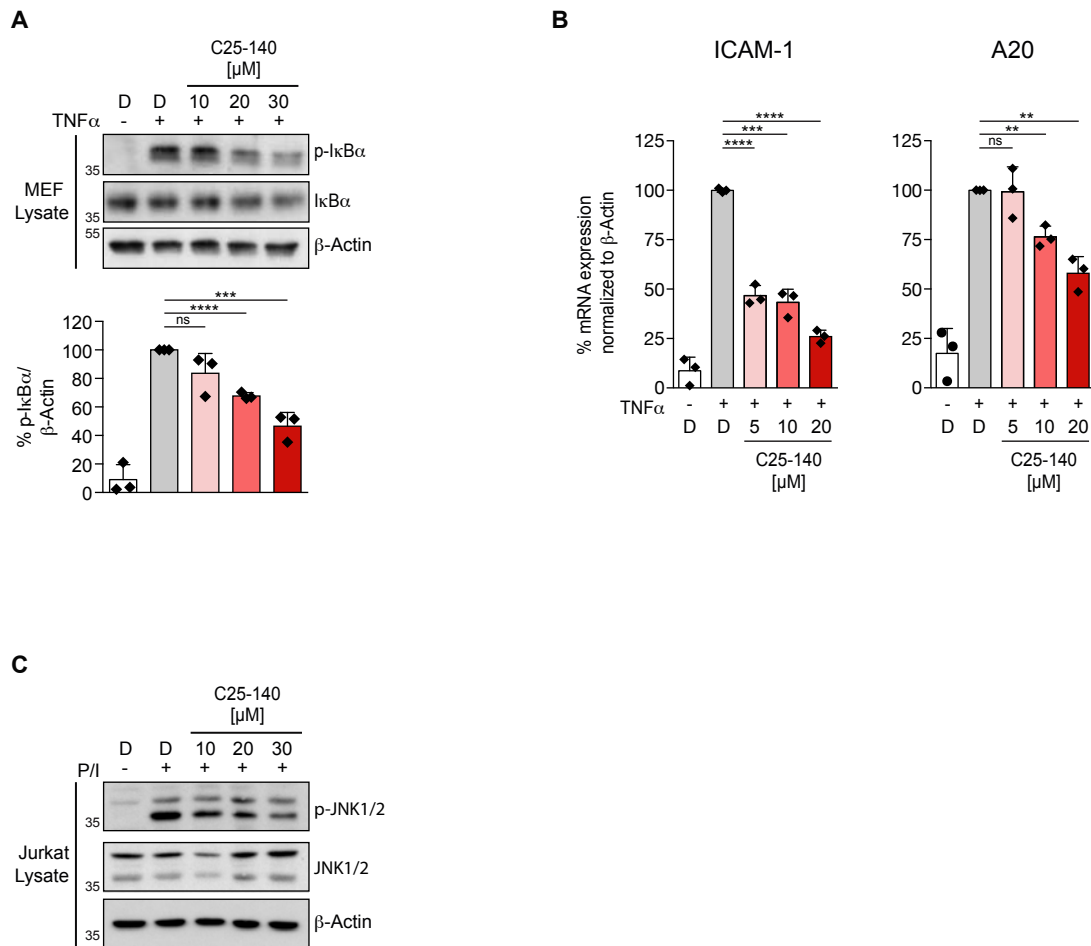


**Figure S4. Effects of C25-140 on TNF $\alpha$ -induced NF- $\kappa$ B activation and P/I-induced MAPK activation.** A, MEF cells were treated with C25-140 and TNF $\alpha$ -induced I $\kappa$ B $\alpha$  phosphorylation was analyzed. C25-140 reduced I $\kappa$ B $\alpha$  phosphorylation. pI $\kappa$ B $\alpha$  levels were densitometrically quantified in relation to  $\beta$ -Actin. Error bars indicate mean  $\pm$  S.D.; n = 3 biological replicates were quantified; unpaired t-test (two-tailed); \*\*\*P<0.001, \*\*\*\*P<0.0001. B, Target gene (ICAM-1 and A20) expression is also diminished after C25-140 treatment and TNF $\alpha$  stimulation. Error bars indicate mean  $\pm$  S.D.; n = 3 biological replicates; unpaired t-test (two-tailed). \*\*P<0.01, \*\*\*P<0.001, \*\*\*\*P<0.0001. C, Jurkat T-cells were treated with C25-140 and P/I-induced JNK phosphorylation was analyzed. C25-140 reduced JNK phosphorylation indicating inhibition of MAPK signaling; D = DMSO

# Figure S5

A

ADME test	Result
Plasma stability [10 $\mu$ M]	$T_{1/2} > 240$ min
Plasma protein binding assay [1 $\mu$ M]	96.8 %
Microsomal stability [2 $\mu$ M]	$K_{el} = 0.004$ /min $T_{1/2} = 171.63$ /min $CL_{int} = 9.73\mu$ L/min/mg
LogD, pH 7.4 (0.1mM in PBS; 1mM in Octanol)	2.83
Caco-2 assay [10 $\mu$ M]	$P_{app} = 48.02 \cdot 10^{-6}$ /cm
CYP450 inhibition [20 $\mu$ M]	CYP1A2: 25.73 % CYP2C9: 94.20 % CYP2C10: 82.53 % CYP2D6: 67.54 % CYP3A4: 45.76 %
hERG binding assay (inhibition)	10 $\mu$ M: 2.1 % 30 $\mu$ M: 26.5 % 50 $\mu$ M: 28.3 %

B

	IV [10mg/kg]	PO [10mg/kg]	IP [10mg/kg]
$T_{max}$	$T_{max} = 5$ min	$T_{max} = 15$ min	$T_{max} = 15$ min
$C_{max}$	$C_{max} = 9.7\mu$ g/mL	$C_{max} = 3.4\mu$ g/mL	$C_{max} = 4.2\mu$ g/mL
$AUC_{0-240}$ min	$AUC = 274083$ ng*min/mL	$AUC = 124034$ ng*min/mL	$AUC = 100000$ ng*min/mL
Mean Residence Time	$MRT_{inf} = 32$ min	$MRT_{inf} = 114$ min	$MRT_{inf} = 53$ min
Elimination half life	$T_{1/2} = 80.62$ min	$T_{1/2} = 127.33$ min	$T_{1/2} = 184$ min
Elimination rate constant	$K_{el} = 0.0086$ /min	$K_{el} = 0.0054$ /min	$K_{el} = 0.0038$ /min
Volume of Distribution	$V_d = 4.13$ L/kg	$V_d = 13.3$ L/kg	$V_d = 25.6$ L/kg
Clearance	$CL = 35.53$ mL/min/kg	$CL = 72.38$ mL/min/kg	$CL = 96.2$ mL/min/kg

C

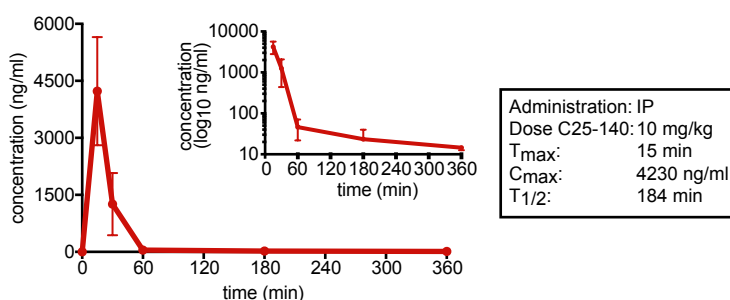


## Figure S5. Absorption/Distribution/Metabolism/Excretion (ADME) properties and pharmacokinetics of C25-140.

A, ADME studies were carried out by determining seven parameters (plasma stability, plasma protein binding, microsomal stability, LogD, Caco-2 permeability assay, CYP450 inhibition and hERG binding assay). C25-140 exhibited appropriate ADME properties: C25-140 was stable in plasma as well as in microsomes, showed favorable oral bioavailability and exhibited low binding to hERG. Only selected CYPs were inhibited. B, Pharmacokinetics (PK) of C25-140 was investigated after intravenous (IV), peroral (PO) and intraperitoneal (IP) injection of mice ( $n = 4$  per sample collection time point and application mode) with 10 mg/kg C25-140 each. Various measurements were evaluated and in total, a rapid initial distribution phase was observed and C25-140 had good calculated oral bioavailability. C, PK curve for IP is illustrated.  $T_{1/2}$ : half time;  $K_{el}$ : elimination rate constant; CL: clearance; MRT: mean residence time;  $V_d$ : volume of distribution.

# Figure S6

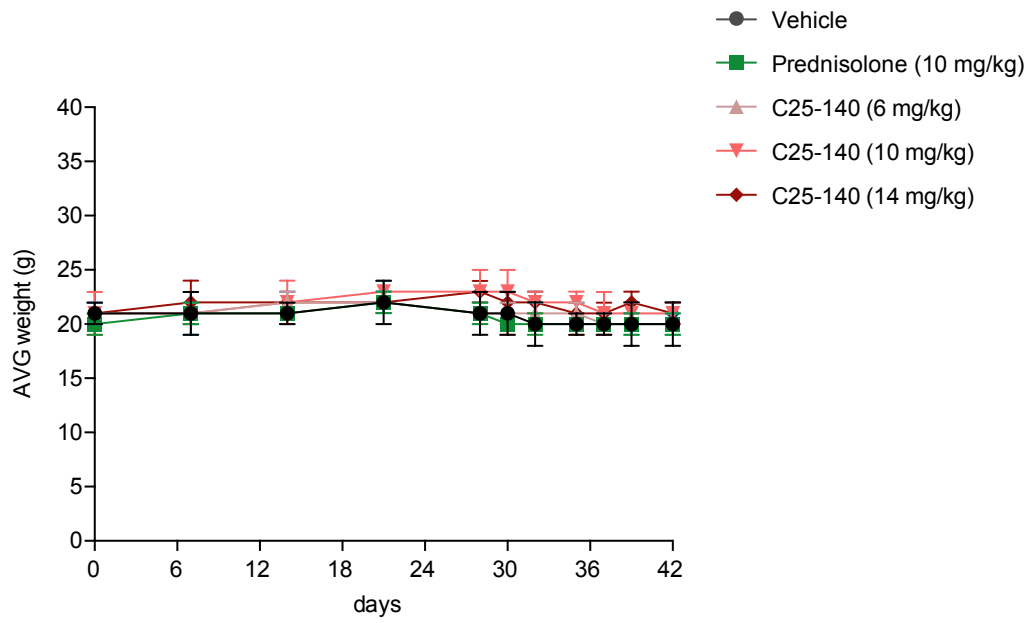


**Figure S6 (referred to Figure 7). Body weight of C25-140 treated mice.** Body weight of all mice (n = 10 per group) was monitored throughout the entire CIA study. No obvious signs of toxicity were detectable for all treatment conditions; error bars indicate mean  $\pm$  S.E.M.



# Figure S7

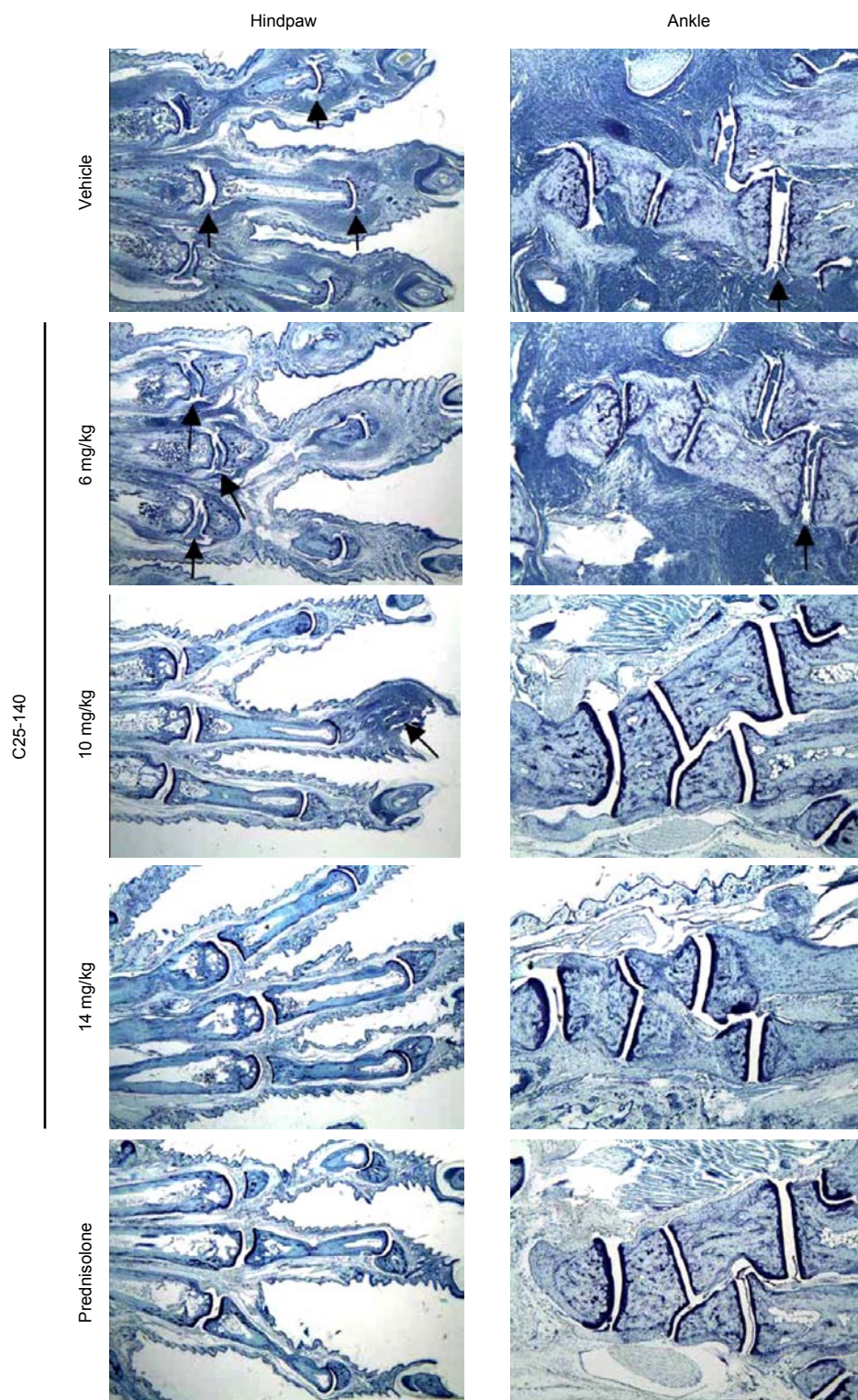


**Figure S7 (referred to Figure 7C). C25-140 ameliorates symptoms of rheumatoid arthritis in a preclinical mouse model.** H&E staining of representative sections of the limbs (hindpaw and ankle) for histopathology are shown for vehicle, three doses of C25-140 and prednisolone. **Vehicle treatment:** Ankle and hindpaw have severe inflammation and cartilage damage, with mild pannus and bone resorption as well as minimal periosteal bone formation in the ankle and all digit joints. Arrows identify representative affected joints. **6 mg/kg C25-140 treatment:** Ankle and hindpaw have severe inflammation and moderate cartilage damage, with very minimal pannus and bone resorption in the ankle and all digit joints. Arrows identify representative affected joints. **10 mg/kg C25-140 treatment:** Ankle and hindpaw have minimal inflammation in a single digit joint. Arrow identifies the affected joint. **14 mg/kg C25-140 treatment:** Ankle and hindpaw have no lesions. **Prednisolone treatment:** Ankle and hindpaw have no lesions.



# Figure S8

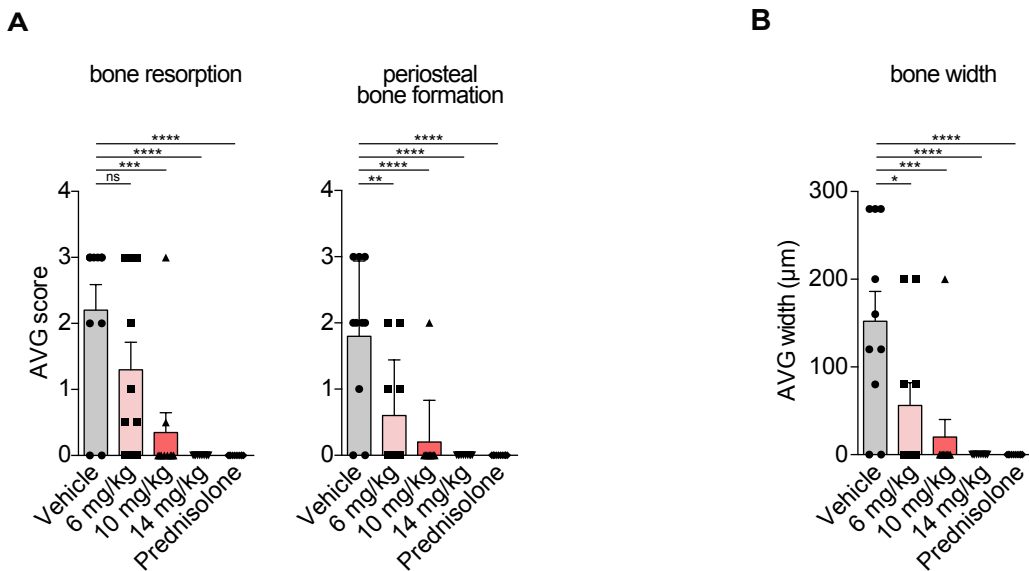


**Figure S8 (referred to Figure 7D-E). C25-140 ameliorates symptoms of rheumatoid arthritis in a preclinical mouse model.** In addition to parameters in Fig. 7D and E, mice were scored for *A*, bone resorption and periosteal bone formation as well as *B*, bone width. These histopathology quantification further demonstrate a dose-dependent improvement of RA symptoms after C25-140 treatment; error bars indicate mean +/- S.E.M.; One-way ANOVA test (Sidak's multiple comparison test).